Vibrational Spectroscopic Studies on Interactions in PEO−NaSCN−Urea Composites

Hucheng Zhang,[†,‡] Xiaopeng Xuan,[†,‡] Jianji Wang,*[,†] and Hanqing Wang[‡]

School of Chemistry & Environmental Science, Henan Normal University, Xinxiang, Henan 453002, P. R. China, and Lanzhou Institute of Chemical Physics, Chinese Academy of Sciences, Lanzhou, Gansu 730000, P. R. China

Received: August 17, 2003; In Final Form: November 27, 2003

FT-Raman (Fourier transform Raman) and FTIR (Fourier transform infrared) studies, along with DTA (differential thermal analysis) and XRD (X-ray diffraction) measurements, were performed on PEO−NaSCN−urea/thiourea solid polymer electrolytes (SPEs) at room temperature, and the interactions of urea/thiourea with NaSCN, PEO, and PEO−NaSCN were analyzed respectively. It is shown that the eutectic molten salt of urea−NaSCN occurs because of the interaction of sulfur in SCN^- with the complex cation formed by the coordination of the N atom in urea with Na^+. Urea and thiourea can form complexes with PEO by hydrogen bonds. When urea is added to PEO−NaSCN SPEs, the formation of such hydrogen bonds and the molten salt of urea−NaSCN causes crystalline PEO and the $P(EO)_3NaSCN$ complex to break up and results in significant changes of the ion association components. In contrast with urea−NaSCN mixtures, the formation of molten salt in thiourea−NaSCN mixtures was not observed and the interactions of thiourea with NaSCN were found to be so weak that the crystal $P(EO)_3NaSCN$ complex could not be broken up in the PEO−NaSCN−thiourea systems. However, the formation of hydrogen bonds and low-melting complexes in the thiourea−PEO systems improves their compatibility and makes the transformation of PEO from the crystalline to the amorphous form possible.

1. Introduction

The use of liquid electrolytes is plagued by leakage problems, so solid electrolytes are envisaged to be most suitable in electrochemical applications. Compared with other solid electrolytes, solid polymer electrolytes (SPEs) have the advantages of having light weight and the required flexibility in design. More notably, SPEs can closely contact the electrode and maintain the contact during changes in volume and under other stresses. Therefore, SPEs have been studied extensively both in industrial and academic intentions.[1−3]

The ether based polymer, poly(ethylene oxide) (PEO), is the most successful host in forming SPEs because of its medium dielectric constant and good electron pair donating ability which makes the host dissolve salt well.[4,5] However, the room-temperature conductivity of PEO-based electrolytes is quite low. It has been shown that improved conductivity can be achieved by increasing the volume fraction of the PEO amorphous phase. Therefore, some ways to disrupt the PEO crystal phase have been employed, which include synthesis of copolymers, comb polymers, and cross-linked polymers, or addition of other polymers and inert inorganic fillers[6−11] such as SiO_2, Al_2O_3, TiO_2, and so forth.

Room-temperature molten salts exhibit desirable electrochemical and material properties such as high electrochemical and thermal stability, high ionic conductivity, low toxicity, and volatility. So, the molten salts and molten salt−polymer electrolytes have been explored for research and development of electrochemical devices.[12−15] It has been shown that urea is able to form molten salts by complexing with several metal ions.[16] Molten salt−polymer electrolytes of urea have also been investigated, and enhancement of conductivity and improvement of electrochemical stability have been reported[17,18] over those of the pure polymer-based systems. However, study of the ion transport mechanism in such SPEs is scarce. Considering the fact that the vibrational stretching modes of SCN^- anions in vibrational absorption spectra vary sensitively with their ionization states, the interactions of urea(U)/thiourea(TU) with PEO, NaSCN, and PEO−NaSCN SPEs were investigated on the basis of their vibrational spectroscopy in this work. Together with differential thermal analysis (DTA) and X-ray diffraction (XRD) measurements, the effect of U/TU content on the ion association and interactions in PEO−NaSCN−U/TU composites is discussed.

2. Experimental Section

PEO ($M_W = 6 \times 10^6$) was a special gift from Liansheng Co. and was dried under vacuum at ~60 °C for 24 h to remove traces of water in the sample. NaSCN (reagent grade, 99.0%) was twice recrystallized in anhydrous ethanol and dried under vacuum at 80 °C for 24 h. Urea and thiourea (99.0%, Beijing Reagent Co.) were recrystallized in deionized water and then vacuum-dried at 45 and 75 °C to constant weigh, respectively. PEO and given amounts of NaSCN and U/TU were mixed with acetonitrile (denoted as AN, 99.9%) and stirred vigorously at room temperature for 24 h until the homogeneous solution was formed. The resulting solution was cast on a Teflon plate and allowed to evaporate slowly inside a desiccator. The films thus obtained were dried in a vacuum for 24 h. The composition of SPEs is represented as $P(EO)_n$NaSCN−y%U/TU, where *n* refers

* Author to whom correspondence should be addressed. Phone: +86-373-3325996. Fax: +86-373-3326445. E-mail: jwang@henannu.edu.cn.
† Henan Normal University.
‡ Chinese Academy of Sciences.

10.1021/jp036447m CCC: $27.50 © 2004 American Chemical Society
Published on Web 01/09/2004

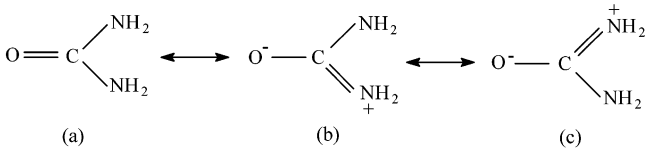

Figure 1. Resonance structures of urea.

to the molar ratio of the ethylene oxide repeating unit and the salt and y% is the weight percent (wt %) of U/TU present in PEO.

The mixtures of NaSCN with urea at the desired molar ratios were heated to an appropriate temperature so that homogeneous liquids were obtained. When cooled to room temperature, the molten salts, whose compositions were expressed as the mole fractions (x) of NaSCN, were sealed in glass capillary tubes for FT-Raman measurements. The FT-Raman spectra were recorded on a Nicolet Thermo FT-Raman spectrometer with a resolution of 2 cm^{-1}.

For infrared measurements the gelatinous polymer solution was cast on a KBr window and then vacuum-dried for 2 h. The infrared absorption spectra were recorded at room temperature on a computer-interfaced Bio-Rad Digilab FTS-40 FTIR spectrometer in the range of 4000−400 cm^{-1} with a resolution of 2 cm^{-1}. Dry N_2 purging gas was used in order to exclude the infrared active H_2O and CO_2 in the atmosphere from the sample chamber.

DTA measurements of composite samples were performed under N_2 purging gas using a Shimadzu DT-40 thermal analyzer. Samples were loaded in sealed aluminum pans, and DTA thermograms were recorded at a heating rate of 10 °C min^{-1}. X-ray diffraction experiments of the composite films were conducted on a Bruker D_8 X-ray diffractometer with Cu Kα radiation and performed at 40 kV and 150 mA with a scan rate of 2 deg min^{-1}.

3. Results and Discussion

3.1. Urea−NaSCN Molten Salt. The urea molecule in the solid state has a planar geometry and a C_{2v} symmetry.[19] It can form complexes with alkaline metals by its three coordination sites: an oxygen and two nitrogen atoms. Because of the conjugation effect between the free electron pairs of the nitrogen atoms and the CO double bond, urea may be represented by a resonance hybrid of three structures as shown in Figure 1. Because the oxygen atom on the urea molecule has a tendency to take a partial negative charge, it is generally thought that the metal−urea complex is formed by the coordination of the oxygen atom in CO with the metal ion.[20] The thiocyanate ion (SCN^-), which is known to resemble halides in its chemical and physical properties, is a linear anion and belongs to the symmetry point group $C_{\infty v}$. Its ambident property makes it possible for it to complex metal ions through the nitrogen or sulfur atom and form N- or S-bonded and bridge complexes,[21−23] depending on the type of metals, the nature of the ligands, and steric effects. Na^+ is a hard acid and has a tendency to bond with the hard base in SCN^- to form an N-bonded compound.

The Raman spectrum of crystalline NaSCN in the range from 2120 to 2020 cm^{-1} (Figure 2) shows that two dominant bands occur at ∼2068 and ∼2077 cm^{-1}. They can be assigned to the internal stretching and external lattice modes of SCN^-.[24] With the increase of urea content in the urea−NaSCN mixture, a new band at ∼2073 cm^{-1} sprouts out at the expense of the bands at ∼2068 and 2077 cm^{-1}. This is associated with the formation of a eutectic molten salt and can be attributed to the SCN^- stretching mode in the urea−NaSCN complex. The new band

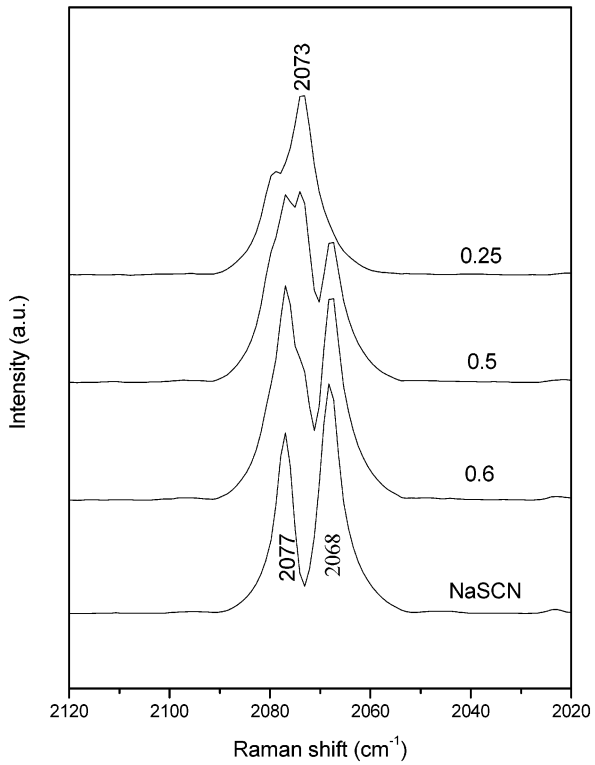

Figure 2. FT-Raman spectra of SCN^- in urea−NaSCN complexes in the region from 2120 to 2020 cm^{-1}. Sample compositions for each curve are given as the mole fraction of NaSCN.

is found to shift toward higher wavenumber by 7 cm^{-1} with respect to the band (at ∼2066 cm^{-1}) for the free SCN^- ion, indicating the formation of the S-bonded complexes in the urea−NaSCN system.[24,25] According to the Lewis acid−base principle, the complex cation formed through the coordination of urea with Na^+ is a polarizable soft acid and is able to bond with the S atom, the soft base in SCN^-. In addition, the band of the CS stretching mode is found to shift from 756 to 753 cm^{-1} and the band of the SCN^- bending mode shifts from 480 to 457 cm^{-1}. These all suggest the formation of S-bonded complexes.[25]

The band at 1010 cm^{-1} can be assigned to the C−N symmetric stretching mode in urea.[26] It is interesting to note from Figure 3 that there are two bands in the range from 1050 to 960 cm^{-1} for the urea−NaSCN mixtures, and the relative intensity of the new band (at 995 cm^{-1}) grows at the expense of the other with the increase of the NaSCN content. When the mole fraction of NaSCN in the mixtures exceeds 0.5, the relative intensities of the two bands keep roughly constant, indicating that the NaSCN content is excessive for the formation of urea−NaSCN complexes. It is possible that the band at 995 cm^{-1} results from the increased single-bond nature of C−N in the urea−NaSCN complex and is an indication of the formation of a Na^+−N-bonded complex. The position of the band at 1010 cm^{-1} was almost unchanged during complexation with respect to that of the C−N stretching for pure urea, suggesting interactions between the SCN^- and the "free" NH_2 groups in urea. The formation of the Na^+−N-bonded complex is also observed in the other region of the Raman spectra as shown in Figure 4. With the increase of the NaSCN content the band of the C−N asymmetry stretching mode at 1467 cm^{-1} shifts toward lower wavenumber, whereas that of the C═O stretching mode at 1540 cm^{-1} shifts significantly toward higher wavenumber. These changes indicate the increased character of the single bond of C−N and the double bond of C═O because of the formation of the Na^+−N-bonded complex. Although the Na^+−O-bonded

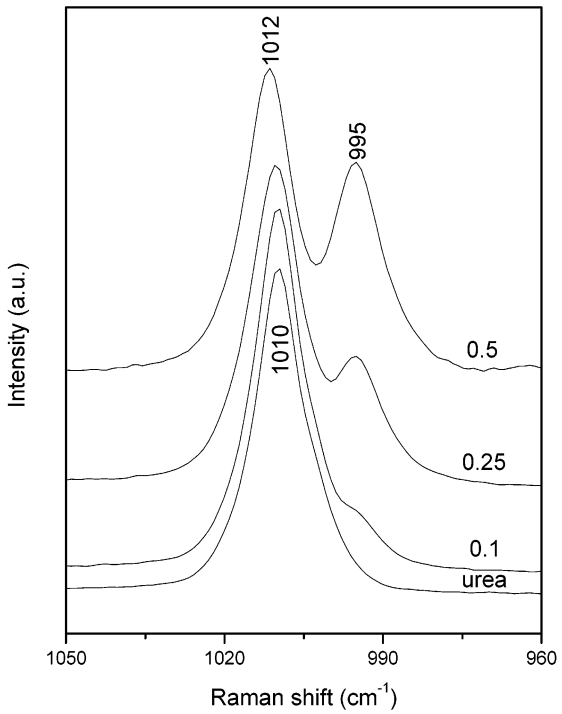

Figure 3. FT-Raman spectra of urea in urea−NaSCN complexes in the region from 1050 to 960 cm^{-1}. Sample compositions for each curve are given as the mole fraction of NaSCN.

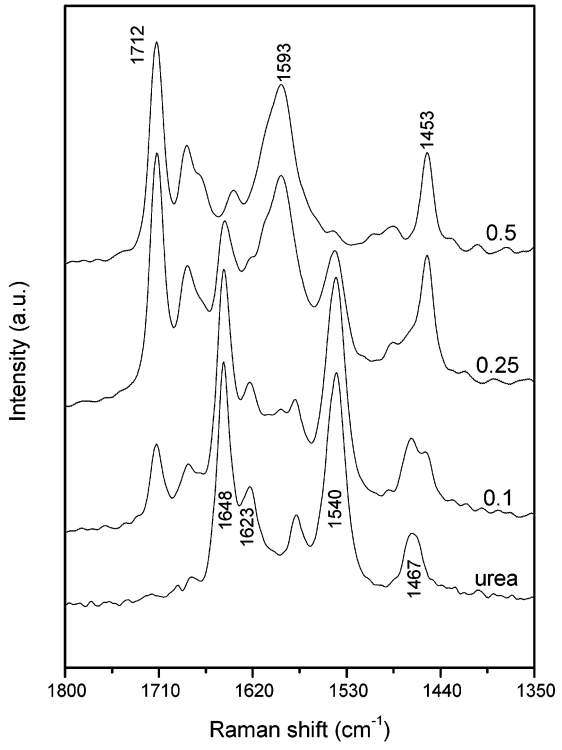

Figure 4. FT-Raman spectra of urea in urea−NaSCN complexes in the region from 1800 to1350 cm^{-1}. Sample compositions for each curve are given as the mole fraction of NaSCN.

complex has been reported, our experiments confirm that it is not the case in the urea−NaSCN system. This is possibly caused by the linear nature of SCN^-, but the exact picture needs to be further studied.

When the urea−NaSCN complex was formed, changes of the N−H vibrational bands were also observed because of the disappearance of hydrogen bonds in solid urea, the coordination of urea with Na^+, and the interactions of SCN^- with NH_2. With

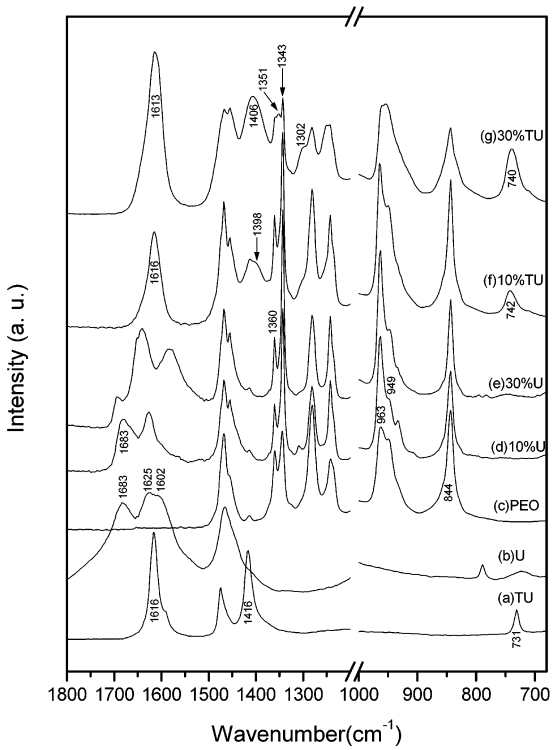

Figure 5. FTIR spectra of PEO−U/TU mixtures in the region of 1800−700 cm^{-1}. Contents for each curve are given as the wt % of U/TU in PEO.

the increase of the NaSCN content, the bands of the NH_2 deformation modes[24] at 1623 and 1648 cm^{-1} shift toward higher wavenumber as shown in Figure 4. The bands of the symmetric N−H stretching modes at 3241 and 3320 cm^{-1} and the asymmetric N−H stretching modes at 3356 and 3429 cm^{-1} in solid urea shift to 3207, 3310, 3366, and 3432 cm^{-1} respectively (not shown) when the mole fraction of NaSCN is 0.5.

Like the urea molecule, thiourea has three resonance forms and can also form complexes with several metal ions. However, it usually coordinates with metals through sulfur.[25] The Raman spectra of thiourea−NaSCN mixtures are found to be just the superposition of the spectra of thiourea and NaSCN, indicating that no complex is formed in the investigated range of the NaSCN mole fraction from 0.05 to 0.7. This phenomenon may result from the inability of the interactions between Na^+ and thiourea to destroy the lattice energy of NaSCN.

3.2. PEO−Urea/Thiourea Mixtures. In the FTIR spectra of PEO as shown in Figure 5 (spectrum c), the bands at 949 and 963 cm^{-1} are assigned to the symmetric and asymmetric CH_2 rocking modes, respectively, and are sensitive to the changes of macromolecular conformations. The bands at 1343 and 1360 cm^{-1} are ascribed to the asymmetric and symmetric CH_2 wagging modes, respectively, and are related to the crystalline phase of PEO.[27,28] With addition of urea to PEO, it is found that the relative intensities of the bands at 963 and 1343 cm^{-1} increase with respect to those at 949 and 1360 cm^{-1} as shown in Figure 5 (spectra c and d), and the C−O−C stretching mode band at 1114 cm^{-1} shifts to 1108 cm^{-1}. At the same time, the FTIR spectra of urea are also changed significantly. The C═O stretching mode[26] band at 1602 cm^{-1} shifts toward higher wavenumber and superposes with the band at 1625 cm^{-1} as seen from Figure 5 (spectra b and d). The bands in the region from 3500 to 3300 cm^{-1}, which are clearly associated with the NH_2 asymmetric and symmetric stretching, shift toward lower wavenumber and become broadened. How-

ever, changes of the bands for the NH_2 deformation modes at 1625 and 1683 cm^{-1} are not significant. On the basis of these observations, it can be deduced that hydrogen bonds occur through the ether oxygen atoms in PEO and the hydrogen atoms in urea and result in changes of the PEO chain conformations. When the urea content is higher than 20%, the bands in the region from 1700 to 1550 cm^{-1} split as shown in Figure 5 (spectrum e) and the bands of the N−H stretching modes in the region from 3500 to 3200 cm^{-1} (not shown) shift to higher wavenumber. This is an indication of the formation of the urea−PEO complex.[29]

When PEO is mixed with thiourea, the changes of the relative intensities of the bands at 963 and 1343 cm^{-1} for PEO are similar to those in the PEO−urea mixtures as shown in Figure 5 (spectrum f). The band at 731 cm^{-1} for thiourea is attributed to the C═S stretching and the C−N stretching modes in which the former is more important than the latter.[30] After complexation of PEO with thiourea, this band shifts to 742 cm^{-1}. The hybrid band at 1416 cm^{-1}, which is assigned to the C═S stretching, the C−N stretching, and the NH_2 rocking modes, shifts to 1398 cm^{-1}. Just like the situation in the PEO−urea system, the bands of the NH_2 stretching modes in the region from 3500 to 3200 cm^{-1} (not shown) shift toward lower wavenumber and become broadened, whereas the band of the NH_2 bending mode at 1616 cm^{-1} remains almost constant. These experimental results indicate also the occurrence of hydrogen bonds between PEO and thiourea. With further increase of the thiourea content, the formation of the PEO−thiourea complex results in the significant changes in the relative intensities of the PEO bands and the shifts of the thiourea bands as seen from Figure 5 (spectrum g). Moreover, the broadened bands of PEO and the new bands at 1302 and 1351 cm^{-1} suggest that the formation of hydrogen bonds and the complexation make also the PEO−thiourea mixtures take amorphous characteristics, that is, the compatibility of thiourea with PEO is better than that of urea with PEO.

Figure 6 presents the DTA thermograms for the PEO−urea/thiourea mixtures. There are two endothermic transitions for the PEO−urea mixtures as shown in Figure 6 (thermograms a and b). The first transition at ∼66 °C corresponds to the melting of the crystalline PEO phase. The second minor endothermic peak at 90 to ∼100 °C is the melting of the PEO−urea complex phase. Two endothermic transitions for PEO−thiourea mixtures are also observed as shown in Figure 6 (thermogram d). The melting temperatures of the crystalline PEO phase and PEO−thiourea complex phase shift to lower temperature compared with those in the PEO−urea system, indicating that the PEO−thiourea mixtures take a more amorphous characteristic and weaker complexation occurs between PEO and thiourea.

3.3. PEO−NaSCN−Urea/Thiourea Composite. The IR stretching mode of SCN^- in $P(EO)_{20}NaSCN$ consists of four bands as shown in Figure 7. Spectroscopically, the band at 2047 cm^{-1} is attributed to free SCN^- and solvent-separated ion-pairs.[31] The band at 2060 cm^{-1} is ascribed to contact ion-pairs and solvent-separated dimers.[32] According to the literature,[32,33] the band at 2081 cm^{-1} is assigned to the triple ion. Along with the occurrence of the band at 2037 cm^{-1}, some new bands of PEO also appear at 826, 835, 853, 922, 1078, 1116, 1137, 1262, 1288, 1352, 1368, and 1475 cm^{-1}. This indicates that NaSCN and PEO form the crystalline complex $P(EO)_3NaSCN$, which is consistent with the conclusion obtained by Dissanayake and Frech.[34] Therefore, it is appropriate to state that the band at 2037 cm^{-1} results from the CN stretching vibration in $P(EO)_3NaSCN$.

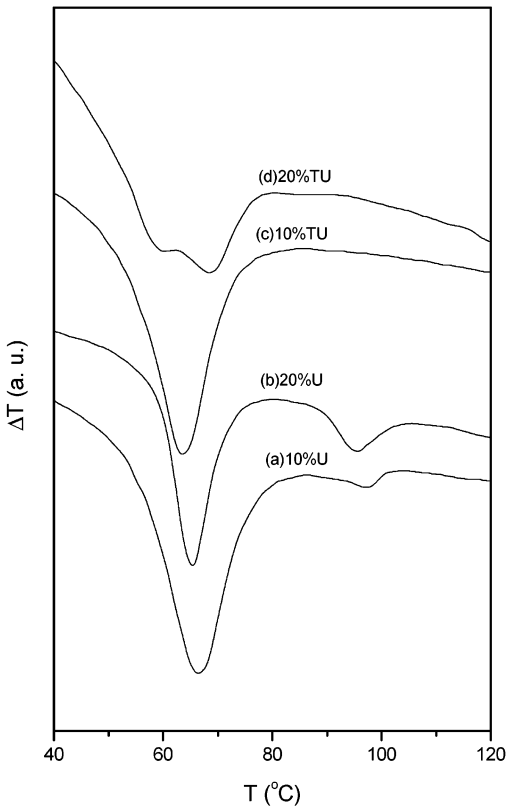

Figure 6. DTA thermograms of PEO−U/TU mixtures. Contents for each curve are given as the wt % of U/TU in PEO.

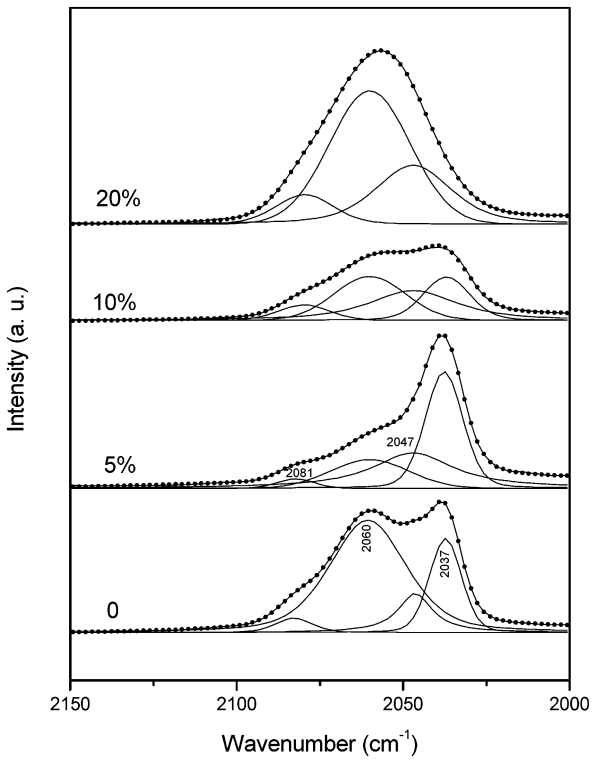

Figure 7. Fitted FTIR spectra of SCN^- in $P(EO)_{20}NaSCN$−y%U in the range of 2150−2000 cm^{-1}. Contents of urea (y%) are indicated in each curve.

To investigate the effect of urea on ion association in PEO−NaSCN SPEs, the spectral envelope in the range from 2150 to 2000 cm^{-1} is curve-fit to a straight baseline and one Gaussian−Lorentzian product function for each band using the Bio-Rad Win-IR software. The curve-fitting results for the

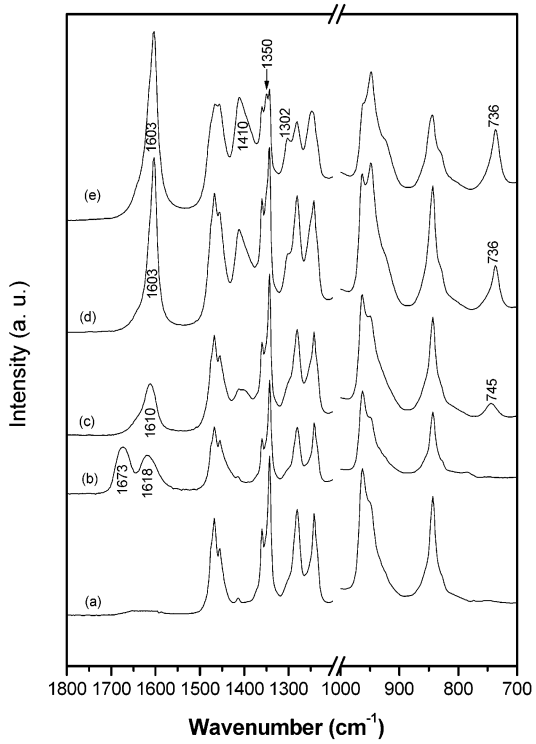

Figure 8. FTIR spectra of $P(EO)_{20}NaSCN-y\%U/TU$ in the 1750−700 cm^{-1} region as a function of U/TU content: spectrum a 0%, spectrum b 10% U, spectrum c 5% TU, spectrum d 10% TU, spectrum e 20% TU.

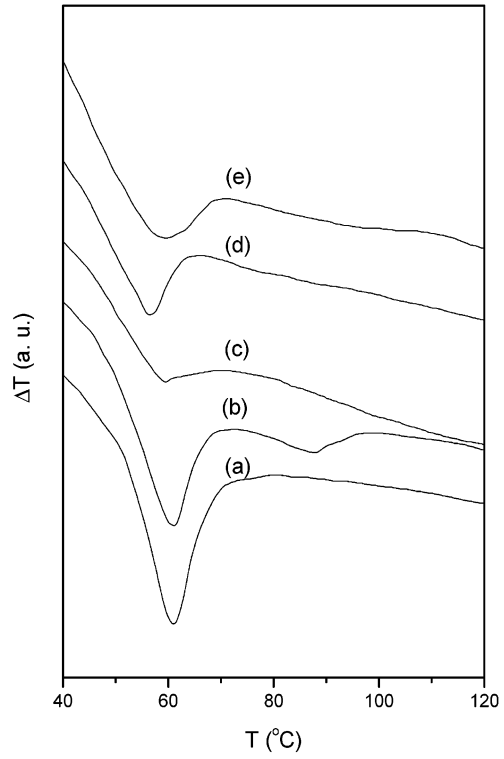

Figure 9. DTA thermograms of PEO−NaSCN−U/TU composites: thermogram a $P(EO)_{20}NaSCN-10\%U$, thermogram b $P(EO)_{20}NaSCN-20\%U$, thermogram c $P(EO)_8NaSCN-20\%U$, thermogram d $P(EO)_{20}NaSCN-10\%TU$, thermogram e $P(EO)_{20}NaSCN-20\%TU$.

$P(EO)_{20}NaSCN-y\%U$ systems are shown in Figure 7. When the content of urea is less than 5%, the relative intensity of the band at 2037 cm^{-1} increases, whereas that of the band at 2060 cm^{-1} decreases with increasing urea content. However, when the urea content exceeds 5%, the relative intensity of the band at 2037 cm^{-1} decreases and that at 2060 cm^{-1} increases. Finally, the bands at 2047 and 2060 cm^{-1} become the dominant components.

Figure 8 (spectrum b) shows that the FTIR spectrum of PEO in $P(EO)_{20}NaSCN-10\%U$ composites is almost the same as that in $P(EO)_{20}NaSCN$ SPE, and this situation is not varied significantly with increasing urea content. However, the changes of the urea spectrum in the composites can be clearly observed. The spectrum of urea exhibits two bands at 1618 and 1673 cm^{-1} in the region from 1700 to 1600 cm^{-1}. The bands of the NH_2 stretching modes at 3450, 3444, 3349, and 3341 cm^{-1}, and the hybrid band of the NH_2 deformation and the C═O stretching at 3264 cm^{-1}, all shift toward lower wavenumber. Moreover, it is found that these changes of the urea spectra do not depend on the contents of urea (from 1% to 30%) and NaSCN (from that in $P(EO)_{80}NaSCN$ SPE to that in $P(EO)_8NaSCN$ SPE), suggesting that all the urea molecules in composites are roughly in the same environment.

It is obvious that there are a number of chemical moieties and possibilities of various interactions in the PEO−NaSCN−urea composites. The properties of such composite systems are a result of a balance of interactions among PEO, NaSCN, and urea molecules. On the basis of the spectroscopic changes of the composites and the fact of dipolar interactions between NaSCN and urea, it is possible that the formation of hydrogen bonds between NH and COC weakens the solvating ability of PEO to Na^+ and increases the negative charges of oxygen atoms in C═O when urea is added to PEO−NaSCN SPEs. Therefore, the addition of urea can enhance the static charge repulsion between $CO^{\delta-}$ and SCN^- and promote the formation of the $P(EO)_3NaSCN$ complex. As the content of urea is increased further, $CO^{\delta-}$ can insert into the ion-pairs of NaSCN to form "solvent-separated" ion-pairs or "solvent-separated" dimers. The former is similar, in structure, to the urea−NaSCN molten salt derived through coordination of the O atom in urea with Na^+ and the latter to "the side chains" attached on PEO backbones. These structures can lead to the destruction of the $P(EO)_3NaSCN$ complex and crystalline PEO, so that the bands at 2047 and 2060 cm^{-1} become the main components. This conclusion may also be confirmed by the addition of urea into the $P(EO)_8NaSCN$ SPE, in which the band at 2037 cm^{-1} is the main component. When the urea content is less than 10%, the band at 2037 cm^{-1} does not change significantly. However, the bands at 2047 and 2060 cm^{-1} become dominant components in the $P(EO)_8NaSCN-30\%U$ system, and all the bands of PEO are broadened. Those facts suggest that those structures formed by urea and PEO−NaSCN SPE can play the role of "plasticizer" in the composites.

As seen from the DTA thermograms a and c in Figure 9, the absence of a minor endothermal peak (around 90 °C) suggests that the PEO−urea complex is repressed because of the interactions of urea with NaSCN. The shallow melting peak of the crystalline PEO phase in Figure 9 (thermogram c) indicates that a very low degree of crystallization of PEO occurs in the $P(EO)_8NaSCN-20\%U$ composite. These conclusions are in good agreement with the results obtained from FTIR spectroscopy studies.

Figure 10 shows the results of curve-fitting the FTIR spectra of $P(EO)_{20}NaSCN-y\%TU$ composites in the region from 2150 to 2000 cm^{-1}. The relative intensity of the band at 2037 cm^{-1} decreases whereas the intensities of the bands at 2047 and 2060 cm^{-1} increase with increasing thiourea content. Because of the weak interactions between PEO and NaSCN, the spectral changes of PEO and thiourea in the SPE are similar to those in PEO−thiourea mixtures as shown in Figure 8 (spectra c through

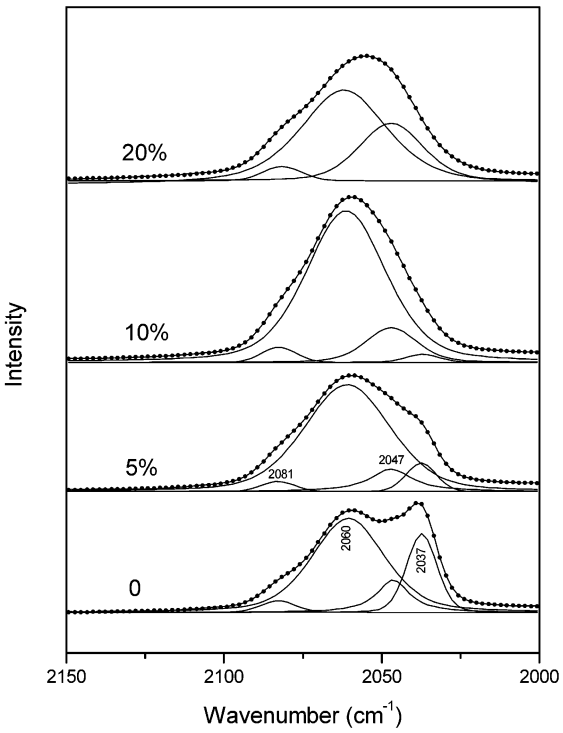

Figure 10. Fitted FTIR spectra of SCN^- in $P(EO)_{20}NaSCN-y\%TU$ in the range of 2150−2000 cm^{-1}. Contents of thiourea (y%) are indicated in each curve.

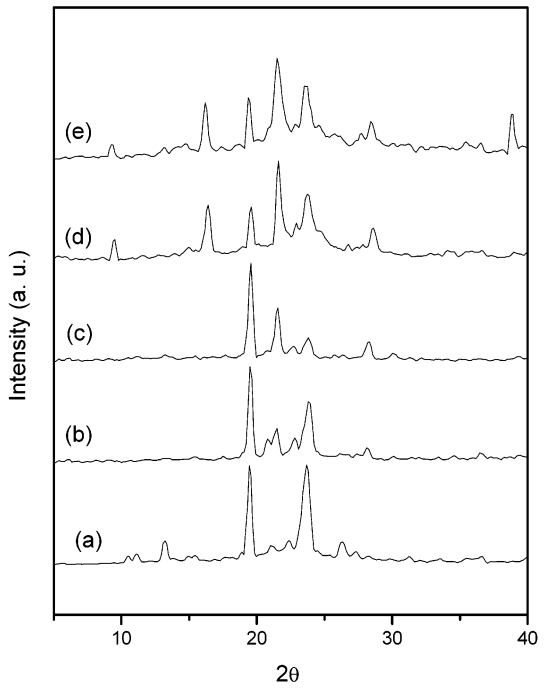

Figure 11. XRD patterns of the samples with the following compositions: diffraction pattern a $P(EO)_{20}NaSCN$, diffraction pattern b PEO−20%U, diffraction pattern c $P(EO)_{20}NaSCN-20\%U$, diffraction pattern d PEO−20%TU, diffraction pattern e $P(EO)_{20}NaSCN-20\%TU$.

e). Therefore, it is possible that the compatibility of thiourea with PEO makes the crystalline phase of PEO transform to an amorphous phase and results in changes of the FTIR spectra in region from 2150 to 2000 cm^{-1}.

However, significant differences in the spectra of the PEO−NaSCN−thiourea composite and the PEO−thiourea mixture are also observed with increasing thiourea content. The relative intensities of the PEO bands in PEO−10%TU (Figure 5 (spectrum f)) are different from those in $P(EO)_{20}NaSCN-10\%TU$ (Figure 8 (spectrum d)), but are similar to those in $P(EO)_{20}NaSCN-5\%TU$ (Figure 8 (spectrum c)). This is possibly caused by the weaker capability of forming hydrogen bonds between thiourea and the ether oxygen of the solvated metal ions, which promotes the complexation of thiourea with uncoordinated PEO in the composite. For the changes of the thiourea spectra, the band at 731 cm^{-1} shifts from 745 cm^{-1} in $P(EO)_{20}NaSCN-5\%TU$ to 736 cm^{-1} in $P(EO)_{20}NaSCN-10\%TU$, whereas the band at 1616 cm^{-1} shifts to 1603 cm^{-1}, and the hybrid band at 1416 cm^{-1} shifts to 1410 cm^{-1} in $P(EO)_{20}NaSCN-10\%TU$. Thereafter, these bands seem to keep constant up to a thiourea content of 50%. Thus, it is suggested that the formation of hydrogen bonds between PEO and thiourea increases the weighting of resonance forms b and c in thiourea, and the complex structures of the molten salt, which are similar to those in the $P(EO)_{20}NaSCN$−urea composite, possibly also occur in the PEO−NaSCN−TU composites. However, such interactions are so weak that the $P(EO)_3NaSCN$ crystalline complexes cannot be broken. This inference can be supported by the fact that the band at 2037 cm^{-1} is still the dominant component when 50% TU is added into the $P(EO)_8NaSCN$ SPE.

The broad melting peak in Figure 9 (thermogram e) indicates that the melting temperature of the PEO−thiourea complex in the composites is lower than that in PEO−thiourea mixtures because of the interactions of thiourea with NaSCN, which is similar to that observed in the PEO−NaSCN−urea composites. As seen from the XRD patterns in Figure 11, when NaSCN is added to PEO−U/TU mixtures, the PEO−NaSCN−TU composites exhibit good amorphous phase. However, significant changes in the XRD patterns are observed when NaSCN is added to the PEO−urea mixtures, suggesting a transition of morphology and stronger interactions between urea and NaSCN.

4. Conclusions

It is generally accepted that the oxygen atom in urea takes partial negative charge and can coordinate with alkaline metals to form urea−metal complexes. However, it is found that NaSCN−urea complexes are formed through Na^+-N bonding from the FT-Raman spectra of NaSCN−urea molten salt. It is possible that one N atom in urea coordinates with Na^+ and causes the cation and anion of NaSCN to be separated by urea in such a complex. As a result, the interactions between the large complex cations and the sulfur in SCN^- lead to the formation of NaSCN−urea molten salt. Although the molecular structure of thiourea is similar to that of urea, thiourea shows weaker interactions with NaSCN, and the formation of a thiourea−NaSCN molten salt is not observed in this work.

Urea or thiourea can form hydrogen bonds and even PEO−urea/thiourea complexes with PEO. When added to PEO−NaSCN SPEs, urea results in an increase of crystalline complexe, $P(EO)_3NaSCN$, because of the hydrogen bonds between urea and PEO and the dipolar interactions between $CO^{\delta-}$ and SCN^-. However, under the condition of high urea content, formation of the structure of the urea molten salt may cause the destruction of crystalline PEO and crystalline complexes in PEO−NaSCN SPEs. Therefore, it is expected that the "polymer-in-salt" electrolytes can be prepared using PEO−NaSCN−urea composites. Compared with urea, thiourea exhibits very weak interactions with PEO and NaSCN in SPEs, and it does not readily break the crystalline complex $P(EO)_3NaSCN$ as urea does. On the other hand, the PEO−thiourea complex has a lower melting temperature than the PEO−urea complex, and thiourea can depress the PEO crystal-

lization through mixing with PEO. Thus, PEO−NaSCN−thiourea composites possess an amorphous characteristic and can be used to prepare "salt-in-polymer" electrolytes.

Acknowledgment. The authors acknowledge financial support from the National Natural Science Foundation of China (Grant No. 29973009) and the Innovation Foundation of Henan Education Department.

References and Notes

(1) Dias, F. B.; Plomp, L.; Veldhuis, J. B. J. *J. Power Sources* **2000**, *88*, 169.
(2) Murata, K.; Lzuchi, S.; Yoshihisa, Y. *Electrochim. Acta* **2000**, *45*, 1501.
(3) Tarasco, J. M.; Armand, M. *Nature* **2001**, *414*, 359.
(4) Quartarone, E.; Mustarelli, P.; Magistris, A. *Solid State Ionics* **1998,** *110*, 1.
(5) Andreev, Y. G.; Bruce, P. G. *Electrochim. Acta* **2000**, *45*, 1417.
(6) Fonseca, C. P.; Neves, S. *J. Power Sources* **2002**, *104*, 85.
(7) Hooper, R.; Lyons, L. J.; Moline, D. A.; West, R. *Organometallics* **1999**, *18*, 3249.
(8) Nishimoto, A.; Agehara, K.; Furuya, N.; Watanabe, T.; Watanabe, M. *Macromolecules* **1999**, *32*, 1541.
(9) Wieczorek, W.; Suck, K.; Florjanczyk, Z.; Stevens, J. R. *J. Phys. Chem.* **1994**, *98*, 6840.
(10) Croce, F.; Appetecchi, G. B.; Persi, L.; Scrosati, B. *Nature* **1998**, *394*, 456.
(11) Marcinek, M.; Bac, A.; Lipka, P.; Zalewska, A.; Zukowska, G.; Borkowska, R.; Wieczorek, W. *J. Phys. Chem. B* **2000**, *104*, 11088.
(12) Fuller, J.; Breda, A. C.; Carlin, R. T. *J. Electrochem. Soc.* **1997**, *144*, L67.
(13) Lagrost, C.; Carrie, D.; Vaultier, M.; Hapiot, P. *J. Phys. Chem. A* **2003**, *107*, 745.
(14) Noda, A.; Susan, M. A. B. H.; Kudo, K.; Mitsushima, S.; Hyamizu, K.; Watanabe, M. *J. Phys. Chem. B* **2003**, *107*, 4024.
(15) Stathatos, E.; Lianos, P.; Zakeeruddin, S. M.; Liska, P.; Gratzel, M. *Chem. Mater.* **2003**, *15*, 1825.
(16) Theophanides, T.; Harvey, P. *Coord. Chem. Rev.* **1987**, *76*, 237.
(17) Zhao, D.; Zhang, X.; Zhou, Q.; Li, H.; Zhang, Y.; Xiong, P. *Chem. J. Chin. Univ.* **1999**, *20*, 768.
(18) Zhao, D.; Zhang, X.; Zhou, Q.; Li, H.; Zhang, Y.; Xiong, P. *Chem. J. Chin. Univ.* **2000**, *21*, 794.
(19) Rousseau, B.; Keuleers, R.; Desseyn, H. O.; Van Alsenoy, C. *J. Phys. Chem. A* **1998**, *102*, 6540.
(20) Liang, H.; Li, H.; Wang, Z.; Wu, F.; Chen, L.; Huang, X. *J. Phys. Chem. B* **2001**, *105*, 9966.
(21) Chabanel, M.; Wang, Z. *J. Phys. Chem.* **1984**, *88*, 1441.
(22) Firman, P.; Xu, M.; Eyring, E. M.; Petrucci, S. *J. Phys. Chem.* **1992**, *96*, 8631.
(23) Xu, M.; Eyring, E. M.; Petrucci, S. *J. Phys. Chem.* **1995**, *99*, 14589.
(24) Lin, C.; Teeters, D.; Potter, W.; Tapp, B.; Sukkar, M. H. *Solid State Ionics* **1996**, *86−88*, 431.
(25) Nakamoto, K. *Infrared and Raman Spectra of Inorganic and Coordination Compounds*; John Wiley and Sons: New York, 1986.
(26) Keuleers, R.; Dessyn, H. O.; Rousseau, B.; Alsenoy, C. V. *J. Phys. Chem. A* **1999**, *103*, 4621.
(27) Wieczorek, W.; Raducha, D.; Zalewska, A.; Stevens, J. R. *J. Phys. Chem. B* **1998**, *102*, 8725.
(28) Papke, B. L.; Ratner, M. A.; Shriver, D. F. *J. Phys. Chem. Solids* **1981**, *42*, 493.
(29) Yan, J. *Water-Solubility Macromolecules*; Chem. Ind.: Beijing, 1998.
(30) Yamaguchi, A.; Penland, P. B.; Mizushima, S.; Lane, T. J.; Curran, C.; Quagliano, J. V. *J. Am. Chem. Soc.* **1958**, *80*, 527.
(31) Irish, D. E.; Tang, S. Y.; Talts, H.; Petrucci, S. *J. Phys. Chem.* **1979**, *83*, 3268.
(32) Saar, D.; Petrucci, P. *J. Phys. Chem.* **1986**, *90*, 3326.
(33) Bacelon, P.; Corset, J.; de Loze, C. *J. Solution Chem.* **1980**, *9*, 129.
(34) Dissanayake, M. A. K. L.; Frech, R. *Macromolecules* **1995**, *28*, 5321.